THE JOURNAL OF BIOLOGICAL CHEMISTRY VOL. 285, NO. 36, pp. 27798–27805, September 3, 2010


# The C*X*C Chemokine-degrading Protease SpyCep of *Streptococcus pyogenes* Promotes Its Uptake into Endothelial Cells*[S]

Received for publication, December 22, 2009, and in revised form, June 10, 2010 Published, JBC Papers in Press, June 18, 2010, DOI 10.1074/jbc.M109.098053

**Simran Jeet Kaur[‡], Andreas Nerlich[‡], Simone Bergmann[‡], Manfred Rohde[‡], Marcus Fulde[‡], Dorothea Zähner[‡1], Emanuel Hanski[§], Annelies Zinkernagel[¶], Victor Nizet[¶], Gursharan S. Chhatwal[‡], and Susanne R. Talay[‡2]**

*From the [‡]Department of Microbial Pathogenesis, Helmholtz Centre for Infection Research, Inhoffenstrasse 7, D-38124 Braunschweig, Germany, the [§]Institute of Microbiology, The Hebrew University-Hadassah Medical School, Jerusalem 91010, Israel, and the [¶]Department of Pediatrics and Skaggs School of Pharmacy and Pharmaceutical Sciences, University of California, San Diego, La Jolla, California 92093*

***Streptococcus pyogenes*** **expresses the LP*X*TG motif-containing cell envelope serine protease SpyCep (also called ScpC, PrtS) that degrades and inactivates the major chemoattractant interleukin 8 (IL-8), thereby impairing host neutrophil recruitment. In this study, we identified a novel function of SpyCep: the ability to mediate uptake into primary human endothelial cells. SpyCep triggered its uptake into endothelial cells but not into human epithelial cells originating from pharynx or lung, indicating an endothelial cell-specific uptake mechanism. SpyCep mediated cellular invasion by an endosomal/lysosomal pathway distinct from the caveolae-mediated invasion pathway of *S. pyogenes*. Recombinant expression and purification of proteolytically active SpyCep and a series of subfragments allowed functional dissection of the domains responsible for endothelial cell invasion and IL-8 degradation. The N-terminal PR domain was sufficient to mediate endothelial cell invasion, whereas for IL-8-degrading activity, the protease domain and the flanking A domain were required. A polyclonal rabbit serum raised against the recombinant protease efficiently blocked the invasion-mediating activity of SpyCep but not its proteolytic function, further indicating that SpyCep-mediated internalization is independent from its enzymatic activity. SpyCep may thus specifically mediate its own uptake as secreted protein into human endothelial cells.**

*Streptococcus pyogenes* is an important human pathogen able to cause infections ranging from mild pharyngitis to severe invasive disease. Necrotizing fasciitis and other life-threatening *S. pyogenes* infections are increasingly reported during recent decades, and large efforts have been undertaken to identify virulence factors that play a role in their development. A genome-wide analysis of the transcriptome of invasive *versus* non-invasive serotype M1T1 *S. pyogenes* strains revealed a frameshift mutation in the global transcriptional regulator sensor gene *covS* among the invasive strains, resulting in the up-regulation of several putative or known virulence factors (1). One such virulence factor was SpyCep (ScpC, PrtS), a subtilisin type serine protease, whose encoding mRNA was more than 10-fold more abundant in the invasive transcriptome. SpyCep is a 1647-amino acid protein and predicted to be secreted and covalently linked to the streptococcal cell wall via a C-terminal LP*X*TG motif. The enzyme shares the overall multidomain organization of cell envelope proteases (Ceps)[3] of lactic acid bacteria, consisting of a pre-pro-domain for Sec-dependent secretion and autocatalytic activation, the PR domain for catalytic activity, and the subsequent A and B/H domains of yet undefined function (2).

Two independent studies identified SpyCep as the key enzyme for IL-8 degradation and impaired neutrophil recruitment (3, 4). The IL-8-degrading enzyme was first isolated from culture supernatant of an invasive M81 isolate. Using this purified enzyme, cleavage of IL-8 between amino acid residues 59 and 60 rendered this major human chemoattractant functionally inactive (3). Subsequently, studies conducted with a highly invasive M14 isolate and a set of isogenic knock-out mutants revealed that SpyCep not only degrades the human C*X*C motif-containing chemokine IL-8 but also the murine chemokines KC and MIP-2 (4). A recent study focused on the role of SpyCep in the globally disseminated M1T1 *S. pyogenes* clone that has emerged as the leading cause of invasive infections during recent epidemiology (5). Using a SpyCep knock-out mutant as well as a *Lactococcus lactis* strain that expressed heterologous SpyCep, it could be demonstrated that SpyCep was necessary and sufficient to impede IL-8-dependent neutrophil endothelial transmigration and also exerted a strong inhibitory effect on neutrophil bacterial killing and extracellular trap formation (5).

The gene encoding SpyCep is present in *S. pyogenes* strains of all serotypes, but expression levels may vary to a large extent. Mutation events such as those affecting SilCR, which encodes a

* This work was supported by Grant VWZN2038 from the Niedersächsisches Ministerium für Wissenschaft und Kultur of Lower Saxony the "Wiedereinstiegsprogramm" given by the Helmholtz Association, Germany (to S. R. T.), and "CAREPNEUMO" (Grant EU-CP223111, European Union) (to S. R. T. and S. B.).

[S] The on-line version of this article (available at http://www.jbc.org) contains supplemental Fig. S1.

[1] Present address: Division of Infectious Diseases, Dept. of Medicine, Emory University School of Medicine, Atlanta, GA.

[2] To whom correspondence should be addressed. Tel.: 49-531-6181-4503; Fax: 49-531-6181-4499; E-mail: susanne.talay@helmholtz-hzi.de.

[3] The abbreviations used are: Cep, cell envelope protease; EC, endothelial cell; HUVEC, human umbilical vein endothelial cells; EEA1, early endosomal antigen 1; EGM-2, endothelial cell growth medium 2; Ni-NTA, nickel-nitrilotriacetic acid; PR domain, protease domain; GBS, group B *Streptococcus*.

regulatory peptide inhibiting SpyCep activity, or CovRS appear to be responsible for the emergence of highly aggressive strains (1, 6–8).

Because SpyCep plays a central role in invasive streptococcal disease by impairing neutrophil recruitment across the vascular endothelium, the endothelial cell represents an important part of the natural environment of SpyCep expression. We thus sought to further characterize the biological function of SpyCep by analyzing its interaction with endothelial cells. We were able to clone, express, and purify full-length recombinant SpyCep in its enzymatically active form. SpyCep was found to mediate its uptake into endothelial cells via an endosomal/lysosomal pathway. Dissection of the functional domains revealed that the SpyCep N-terminal PR domain mediated uptake into endothelial cells, whereas the PR+A domain was required for IL-8-degrading activity.

## EXPERIMENTAL PROCEDURES

*Bacterial Strains and Culture Conditions*—*S. pyogenes* strains were grown overnight in Todd Hewitt Broth (Oxoid) containing 5% yeast extract. The invasive M14 *S. pyogenes* strain JS95 as well as its isogenic SpyCep deletion mutant JS95 ΔscpC/ΔscpA were described earlier (4). The *S. pyogenes* strain A475 is an invasive serotype M3 isolate, and the SpyCep mutant strain A475 ΔSpyCep was grown in the presence of 80 μg/ml spectinomycin. *Streptococcus agalactiae* serotype Ia strain 102 served as a recipient for the vector pDCerm or the SpyCep-expressing plasmid p*cepA*, which were described previously (5).

*Cloning, Expression, and Purification of SpyCep from Escherichia coli*—For expression of the full-length mature form of SpyCep (rSpyCep, ranging from amino acids 111 to 1560 according to accession number ABA33824.1), excluding the N-terminal pre-pro-domain and the C-terminal cell wall-anchoring domain, a DNA fragment spanning nucleotides 658–5008 of the *scpC* gene (accession number DQ192030) was amplified. Primers for amplification (Expand high fidelity PCR system) were: rSpyCep forward, 5′-GCTAATTCATGACTGATGCGACTCAA-3′, and rSpyCep reverse, 5′-TTCATTGGATCC-GGTATTCACCTTTG-3′. Following digestion with BspHI and BamHI, the amplicon was cloned into the NcoI/BamHI-digested vector pQE-60 (Qiagen) using standard cloning procedures. For cloning and expression of SpyCep subdomains PR (spanning amino acids 111–685) and PR+A (spanning amino acids 111–1125), the following reverse primers were used in combination with the above listed forward primer: PR reverse, 5′-CCGCTGGATCCAGCTCCGTCAATATT-3′, and PR+A reverse, 5′-CGGATCCTTGTGGTGGTAGGTGATCTCCT-3′. The resulting constructs expressed polypeptides with a C-terminal histidine tag that allowed purification using Ni-NTA agarose under native conditions according to standard procedures (Qiagen). The SpyCep A domain, ranging from amino acids 691 to 1127 (according to accession number ABA33824.1), and the A+B/H domain, ranging from amino acids 691 to 1560, were expressed as recombinant fusion proteins tagged with glutathione *S*-transferase (GST). DNA fragments were amplified with the following primers: A domain forward, 5′-CGGGATCCTATGTGACAGGAAAAGAC-3′; A domain reverse, 5′-CCGGAATTCTCATGTTTGTGGTAGGTGATC-3′; and A+B/H domain reverse, 5′-CGGGAATTCTCAGGTATTCACCTTTGTGTT-3′ and cloned into pGEX-6P-1 according to standard cloning procedures. Expression of GST-tagged SpyCep polypeptides and subsequent purification using glutathione-Sepharose affinity chromatography was conducted according to the manufacturer's protocol.

*Construction of a SpyCep Knock-out Mutant in S. pyogenes A475*—An allelic exchange strategy (9) was used to create a SpyCep deletion mutant in the serotype M3 strain *S. pyogenes* A475. Briefly, a 514-bp fragment of the 5′ region of the *scpC* gene ranging from nucleotides 47 to 561 was amplified using primers scpC1 (5′-CGTTTTCGGTCTTA-ATAGGAAGCG-3′) and scpC3 (5′-CCGGGCAATTGCCGGGATTAAT-ACCGGCGGCTTTTTGG-3′), and a 535-bp fragment of the 3′ region was amplified ranging from nucleotides 1625 to 2160 using primers scpC2 (5′-AACAGTCACATCAAACGTCATCG-3′) and scpC4 (5′-GCCGCGCCTAGGCGCACGAATTTGGTAAGGCCATGTC-3′). In addition, the spectinomycin resistance cassette (spc) was amplified using primers spc1 (5′-CCCGGCAATTGCCCGGATCGATTTTCGTTCGTGAAT-3′) and spc2 (5′-GCGCCTAGGCGCGGCCCAATTAGAATGAATATTTCCC-3). All three PCR fragments were used as templates in a single PCR-based overlap extension reaction using primers scpC1 and scpC2. The resulting PCR product, consisting of the spc cassette and flanking *scpC* regions, was cloned into vector pCR2.1 using the TOPO TA cloning kit (Invitrogen). After cleavage with BamHI/XhoI, the insert was cloned into the temperature-sensitive shuttle vector pJRS233 (9), resulting in plasmid pCEP-KO. *S. pyogenes* A475 was transformed with pCEP-KO by electroporation, and transformants were selected on Todd Hewitt Broth (Oxoid) containing 5% yeast extract containing 1 μg/ml erythromycin at 30 °C to allow plasmid replication. Integration of the plasmid into the chromosome was selected for by a temperature shift to 37 °C. The obtained clones were tested for double crossover, leading to the replacement of an internal *scpC* fragment through the spc cassette and a loss-of-function of SpyCep in the deletion mutant.

*Reagents and Antibodies*—Polyclonal antibodies recognizing *S. pyogenes* (anti-group A streptococci) were produced in rabbit as described previously (10). A mouse monoclonal antibody recognizing a luminal epitope of human Lamp-1 (clone H4A3) was purchased from Pharmingen. Secondary goat anti-rabbit IgG antibodies coupled to Alexa Fluor® 488/568 and goat anti-mouse IgG coupled to Alexa Fluor 488 were obtained from Invitrogen (Göttingen, Germany). To raise antibodies against recombinant full-length SpyCep, a rabbit was immunized four times with 100 μg of rSpyCep per dose at 1-week intervals, and serum was collected 2 weeks after the final immunization. For purification of anti-SpyCep IgG antibodies from serum, a column was packed with protein-A-Sepharose CL-4B and equilibrated with 0.1 M potassium phosphate buffer (pH 7.0). Then, 2 ml of rabbit immune serum were applied to the column. The column was washed with PBS, and bound IgG was eluted using 0.1 M glycine/HCl (pH 3.0). The eluate was neutralized by adding 50 μl of Tris-HCl (pH 8.0) to 1 ml of eluate. IgG-containing fractions were pooled, dialyzed against PBS for 16 h, and stored at −20 °C.

*Enzyme-linked Immunosorbent Assay (ELISA)*—Streptococci were grown to mid-exponential phase at 37 °C and collected by centrifugation, and the pellet was washed twice with PBS and then resuspended in Dulbecco's modified essential medium (DMEM; PAA Laboratories) supplemented with 0.1% fetal bovine serum (FBS) and incubated overnight at 37 °C. After centrifugation of the culture, the supernatant was transferred to a 15-ml tube and filtered using a filter with 0.2 $\mu$m-pore size. 50 $\mu$l of the supernatant were diluted to a final volume of 100 $\mu$l with PBS, and 10 ng of IL-8 were added. For testing the activity of recombinant proteins, 5 $\mu$g of recombinant protein were added to 10 ng of recombinant IL-8, and PBS was added to give a final volume of 100 $\mu$l. The reaction mixture was incubated for 16–18 h at 37 °C. The amount of residual interleukin-8 was measured by ELISA using the human IL-8 Quantikine ELISA kit (R&D) according to the manufacturer's instructions. The absorption was measured at 450 nm using an ELISA reader (Tecan Sunrise). For inhibition assays, the culture supernatant of *S. pyogenes* or rSpyCep was incubated with affinity-purified anti-SpyCep IgG (50 $\mu$g/ml) for 1 h at 20 °C and then co-incubated with recombinant IL-8 at 37 °C for 16 h. The residual IL-8 was measured by ELISA as described above.

*Preparation of SpyCep-coated Polystyrene Beads*—For coating polystyrene beads with SpyCep, ~$10^7$ beads (3- and 1-$\mu$m diameter; Sigma) were washed three times in PBS and then coated overnight at 4 °C with 100 $\mu$g/ml of the recombinant mature full-length SpyCep (rSpyCep) or fusion protein constructs containing defined domains of SpyCep (PR, PR+A, and A+B/H). Affinity-purified recombinant GST served as a negative control. Protein-coated beads were washed three times with PBS, collected by centrifugation at 2500 rpm, and finally resuspended in EGM-2 medium supplemented with 2% fetal calf serum (FCS). The coupling efficiency of recombinant protein on beads was analyzed by SDS-PAGE. Briefly, protein was eluted from beads by suspending beads in SDS-PAGE loading buffer and boiling for 5 min. Polypeptides were separated by SDS-PAGE, and the amount of protein was determined by Coomassie Blue staining of the gel. The IL-8-degrading activity of bead-coupled SpyCep was determined via the IL-8 Quantikine ELISA kit according to manufacturer's instructions.

*Endothelial Cell Culture and Internalization Assay*—Primary human large vascular endothelial cells (HUVEC) isolated from umbilical cord were purchased from PromoCell (Heidelberg, Germany). Endothelial cells were cultured and propagated with a maximum of three passages in EGM-2 medium (PromoCell) according to the supplier's protocol in a cell incubator at 37 °C and 5% $CO_2$. Cells were seeded on coverslips in multiwell plates (Nunc, Roskilde, Denmark) and grown to 75% confluency. SpyCep-coated polystyrene beads or SpyCep-coated gold particles were suspended in prewarmed EGM-2 medium and added to endothelial cells with a multiplicity of infection of 100 or 1000, respectively. Alternatively, $10^7$ cfu of SpyCep-expressing *S. agalactiae* (GBS-SpyCep) or *S. agalactiae* containing the vector (GBS-pDCerm) were added per well. Incubation was stopped by washing the monolayer with EGM-2 medium and fixing with PBS containing 4% paraformaldehyde. Distinct time points for fixation were used for monitoring early entry (60–120 min after infection) or subsequent trafficking (120–240 min after infection), respectively.

*Immunofluorescence and Confocal Microscopy*—Endothelial cells that were co-incubated with SpyCep-coated beads were fixed as described above, and samples were blocked for 30 min with PBS containing 10% FCS. Extracellular adherent SpyCep-coated beads were visualized using rabbit polyclonal anti-SpyCep IgG and anti-rabbit Alexa Fluor 488-conjugated IgG. Following permeabilization with 0.01% Triton X-100, extra- and intracellular beads were detected by incubation with anti-SpyCep IgG followed by an Alexa Fluor 568-conjugated anti-rabbit antibody. According to their respective label, intracellular beads appear red, and extracellular beads appear yellow to green. For visualization of F-actin, cells were permeabilized, and F-actin was stained with phalloidin Alexa Fluor 488 for 30 min at room temperature. For early endosomal antigen 1 (EEA1) staining, all incubation steps were performed in 0.05% (w/v) saponin/PBS. Anti-EEA1 (mouse clone 14, BD Biosciences) monoclonal antibody was used 1:25. The bound primary antibodies were visualized with Alexa Fluor 568-conjugated goat anti-mouse IgG. For Lamp-1 analysis, cells were permeabilized and labeled with a mouse anti-human Lamp-1 antibody and a respective anti-mouse Alexa Fluor 488 secondary antibody as described (11). Endothelial cells that were infected with recombinant *S. agalactiae* strains were fixed and stained for extra- and intracellular bacteria using a polyclonal mouse anti-GBS antibody (Acris Antibodies, Herford, Germany) in combination with an anti-rabbit Alexa Fluor 488- or Alexa Fluor 568-labeled secondary antibody, respectively. Coverslips were mounted on glass slides using ProLong® Gold antifade reagent (Molecular Probes). Mounted samples were examined using a Zeiss LSM 510 Meta (Zeiss, Jena, Germany) confocal laser scanning microscope equipped with a 40 × 1.3 NA Plan NEOFLUAR objective (Zeiss). All images were deconvolved using Huygens® Essential (Scientific Volume Imaging, Hilversum, The Netherlands) and processed for contrast and brightness with ImageJ.

*Field Emission Scanning Electron Microscopy*—For field emission scanning electron microscopy, HUVEC were cultivated and co-incubated with protein-coated latex beads (3 $\mu$m; approx. $10^8$ beads) for 2 h at 37 °C under a humidified environment containing 5% $CO_2$. Cells were washed three times with EGM-2 basal medium, fixed with 5% formaldehyde and 2% glutaraldehyde in cacodylate buffer, and prepared for electron microscopic analysis as described (12). Images were recorded digitally with a slow-scan CCD camera (ProScan, 1024 × 1024, Scheuring, Germany) with ITEM software (Olympus Soft Imaging Solutions, Münster, Germany). Brightness and contrast were adjusted with Adobe Photoshop CS3.

*Preparation of SpyCep-Gold Particles*—A solution of colloidal gold with a particle size of 15 nm was coupled to recombinant SpyCep using a coupling method as described (11). SpyCep-gold particles were washed three times in EGM-2 medium, and 50 $\mu$l of the gold particle solution were added to HUVE cells. Adherence and internalization of SpyCep-gold particles to and into HUVEC were monitored as for the SpyCep-coated polystyrene beads.

*Invasion Inhibition Experiments*—For testing the invasion-inhibiting potential of anti-SpyCep antibodies, HUVEC were grown on coverslips as described above. On the day of infection, endothelial cells were washed once in EGM-2 medium containing 5% FCS. SpyCep-coated beads were preincubated with anti-SpyCep polyclonal rabbit IgG or non-immune rabbit IgG as control at a final concentration of 10 $\mu$g/ml for 1 h. Cells were then co-incubated with beads and processed as described above. For determination of uptake rates, intracellular beads were differentially stained as described above and counted using a fluorescence microscope. Intracellular beads of at least 100 cells were determined, and uptake rates were expressed as number of intracellular beads per cell. Experiments were conducted in triplicate on two different days; data presented here resulted from one representative experiment.

*Quantification of SpyCep Surface Localization by Flow Cytometry*—Streptococcal strains were grown to mid-exponential phase in tryptic soy broth medium and washed once in PBS. A total of $1 \times 10^7$ bacteria were suspended in 400 $\mu$l of PBS containing 0.5% FCS and incubated with 0.5 $\mu$g of anti-SpyCep rabbit IgG for 30 min at 37 °C. After washing in PBS, the bacterial pellet was suspended in 100 $\mu$l of PBS containing a 1:300 dilution of an anti-rabbit Alexa Fluor 488 antibody (Invitrogen) and incubated for 30 min at 37 °C. Bacteria were washed in PBS, fixed in PBS containing 3% paraformaldehyde, and analyzed by flow cytometry using a FACSCalibur (BD Biosciences). Streptococci were detected using log-forward and log-side scatter dot plots, and a gating region was set to exclude debris and larger aggregates of bacteria. $10^4$ bacteria were analyzed for fluorescence using log-scale amplification. For detection of SpyCep on latex beads, $1 \times 10^7$ SpyCep-coupled beads were incubated with the respective antibodies and analyzed as described above.

## RESULTS

*Cloning, Expression, and Purification of Enzymatically Active SpyCep*—The *scpC* (SpyCep-encoding) gene encodes a 1647-amino acid protein with an approximate molecular mass of 150 kDa. To be able to perform functional studies with this important virulence factor, we used an *E. coli* expression system to generate and purify a C-terminal hexahistidine ($His_6$) affinity-tagged SpyCep in its biologically active form. Western blotting for direct detection of the fusion protein recognized a band with the anticipated molecular mass of ~150 kDa in the cell lysate of *E. coli* transformants (Fig. 1*A*), indicating expression of mature full-length rSpyCep. rSpyCep was purified from the bacterial cell lysate under native conditions by using immobilized Ni-NTA affinity chromatography (Fig. 1*B*). To determine the IL-8-degrading activity of rSpyCep, a degradation assay based on the quantification of IL-8 via the Quantikine kit was conducted. The culture supernatant of the invasive *S. pyogenes* strain A475 served as a positive control for IL-8 degradation, and its isogenic SpyCep deletion mutant (A475 ΔSpyCep) was used as a negative control. As shown in Fig. 1*C*, rSpyCep efficiently degraded IL-8, as did the culture supernatant of the WT *S. pyogenes* strain, whereas the ΔSpyCep mutant strain lacked IL-8-degrading activity. The IL-8-degrading activity of rSpyCep was further confirmed by Western blot analysis (Fig. 1*D*). These

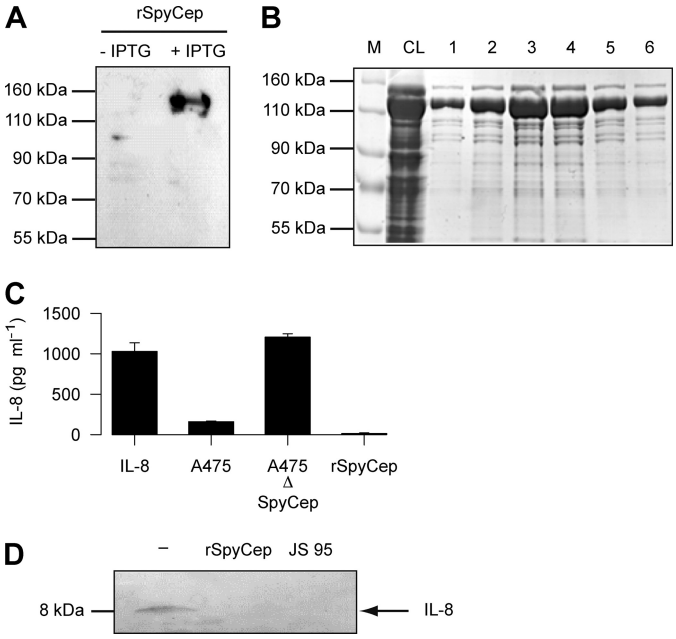


FIGURE 1. **Cloning and recombinant expression of functionally active SpyCep.** *A*, *E. coli* cells transformed with pQE60 derivative expressing full-length mature rSpyCep were induced with IPTG, lysed, and separated via SDS-PAGE. Following transfer to a nitrocellulose membrane, rSpyCep was visualized using a Ni-NTA horseradish peroxidase conjugate for direct detection of the histidine tag. *B*, SDS-PAGE analysis of the *E. coli* cell lysate (*CL*) showing the expression of rSpyCep with molecular mass of ~120–150 kDa. *Lanes 1*-6 refer to the fractions collected after purification of rSpyCep from bacterial crude extracts using Ni-NTA agarose. *M*, molecular mass markers. *C*, quantitative IL-8 degradation assay using the human IL-8 Quantikine ELISA kit. Uncleaved IL-8 and IL-8 incubated with the culture supernatant of the SpyCep knock-out mutant of strain A475 served as negative control, whereas incubation of IL-8 with the supernatant of the *S. pyogenes* WT strain A475 served as positive control for IL-8 cleavage. 5 ng of rSpyCep were capable of degrading IL-8. The graph shows mean values of three independent experiments; the graph represents mean ± S.D. *D*, visualization of rSpyCep-mediated IL-8 degradation by Western blot analysis using an anti-human IL-8 monoclonal antibody that recognizes only full-length IL-8. *S. pyogenes* JS95 culture supernatant served a positive control.

data demonstrate the successful cloning, expression, and purification of full-length mature SpyCep in its functionally active form.

*Functional Dissection of the Domains Required for IL-8-degrading Activity*—To functionally dissect the SpyCep domains responsible for IL-8 degradation, three derivatives of rSpyCep were generated based on the domain structure described for cell envelope serine proteases of lactic acid bacteria (2). Fig. 2 shows the recombinant purified subfragments of SpyCep. Two C-terminally truncated variants of the active rSpyCep were generated: PR+A and PR. In addition, one N-terminally truncated fragment encompassing the A+B/H domain but lacking the PR domain was generated. Using Quantikine ELISA for determination of the IL-8-degrading activity of the purified proteins, the minimal region required for efficient IL-8 degradation was demonstrated to be PR+A (Fig. 2*B*). Neither the PR domain alone, predicted to harbor the catalytic triad of the serine protease, nor the A+B/H domain was able to cleave IL-8.

*SpyCep Mediates Specific Uptake into Primary Human Endothelial Cells*—SpyCep is most likely expressed during soft tissue infection as demonstrated by a reduction of chemokines in infected tissue (4). We thus aimed to analyze potential direct

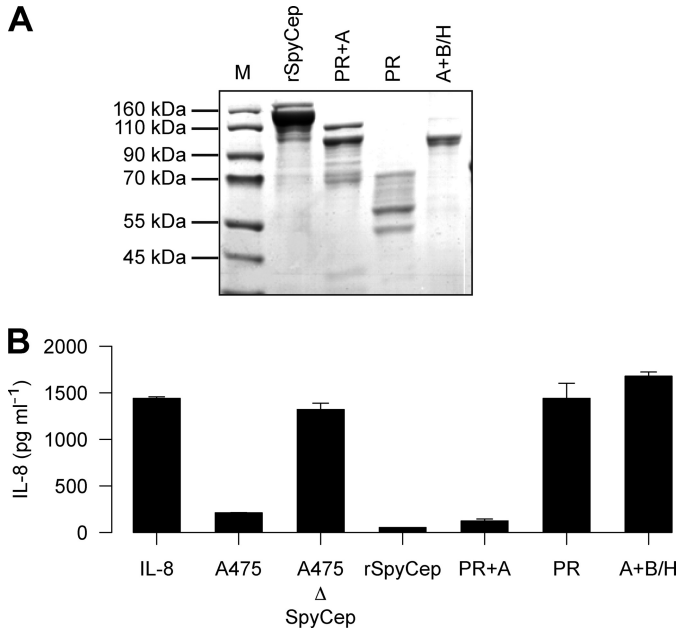


FIGURE 2. **Recombinant expression and functional dissection of SpyCep subdomains.** *A*, Coomassie Blue-stained SDS-PAGE after expression and purification of PR+A, PR, and A+B/H domain of SpyCep. *M*, molecular mass markers. *B*, IL-8-degrading activity of rSpyCep and its subdomains as determined by IL8-Quantikine ELISA. Graph represents mean ± S.D.

interactions of SpyCep with eukaryotic cells of human origin. Because *S. pyogenes* expresses a diverse array of adhesive and invasive factors on its surface, we adopted a latex bead adherence/internalization assay to allow analysis of recombinant SpyCep polypeptides in isolation. Latex beads coated with rSpyCep did not show any adherence or internalization potential on either pharynx (HEp2) or lung (A549) epithelial cells (data not shown). However, in contrast to the epithelial cell findings, rSpyCep-coated beads efficiently attached to and became internalized into primary HUVEC within 2 h of coincubation (Fig. 3*A*). Internalization was observed to be very efficient in some cells, with up to 40 internalized beads per cell, but we simultaneously observed completely empty cells, leading to a mean internalization rate of 32 beads per 10 cells. Next, we aimed to identify the internalization-mediating domain of SpyCep. The recombinant PR polypeptide, representing the N-terminal part of SpyCep, and the A+B/H polypeptide, representing the residual C-terminal part of SpyCep, were tested for internalization-mediating activity in the latex bead assay. Quantification of internalization rates revealed that the PR domain of SpyCep was sufficient to mediate internalization into endothelial cells, whereas the residual part of SpyCep did not stimulate internalization beyond background control levels (Fig. 3*B*). Ultrastructural analysis by electron microscopy revealed that SpyCep stimulated the formation of membrane protrusions on the endothelial cell surface (Fig. 4, *A–D*). On the cytoskeletal level, SpyCep-coated beads induced the formation of F-actin-rich structures engulfing the beads (Fig. 4, *E* and *F*, *arrows*). These results demonstrate that SpyCep mediates an endothelial cell-specific uptake and that the N-terminal PR domain is both essential and sufficient for triggering uptake, although it lacks IL-8-degrading activity.

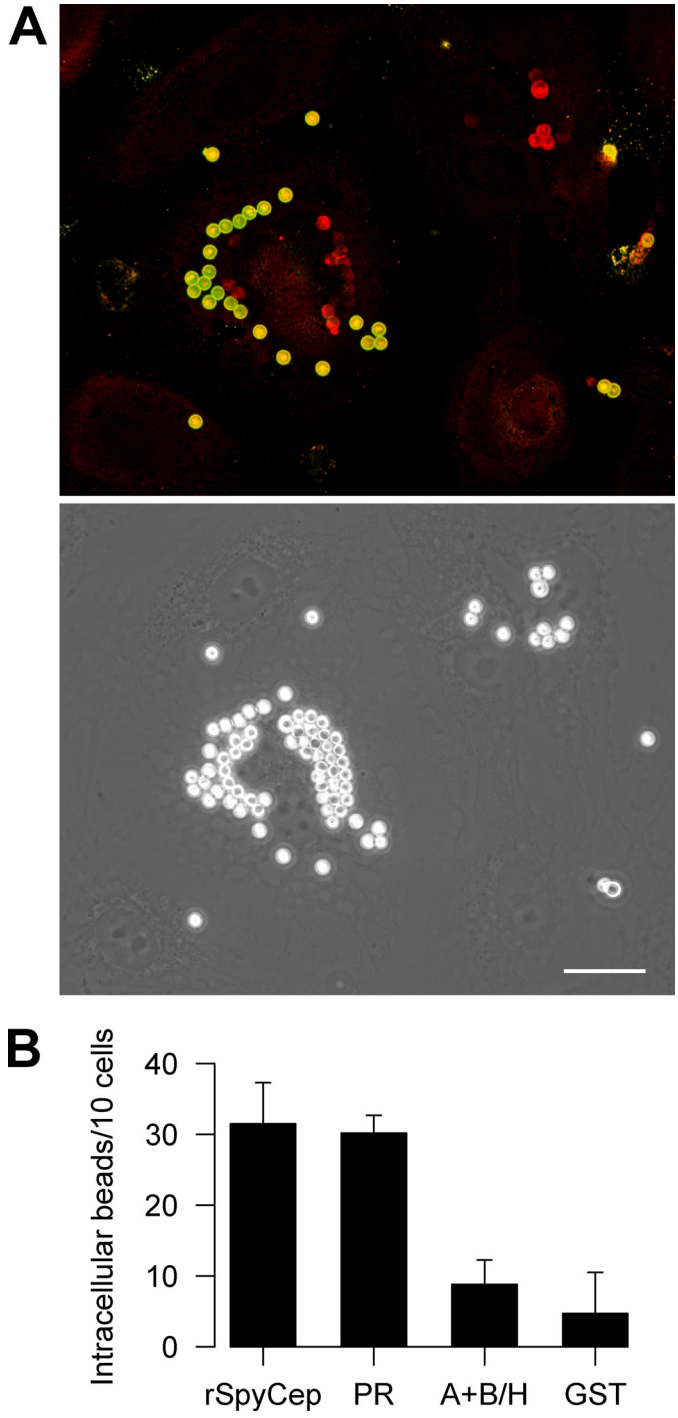


FIGURE 3. **SpyCep mediates internalization of SpyCep-coated beads into HUVEC.** *A*, confocal maximum intensity projection of a double immunofluorescence staining of HUVEC with extracellular attached (*green*) and intracellular (*red*) SpyCep-coated beads and the corresponding phase contrast image. Note that a substantial number of internalized beads are no longer stained by the anti-SpyCep antibody, indicating loss of SpyCep, and thus are only visible in the phase contrast image. *Bar* represents 10 μm. *B*, comparison of bead internalization rates into HUVEC. SpyCep-coated beads served as positive control, and GST-coated beads serve as negative control. Graph represents mean ± S.D.

*SpyCep-mediated Uptake Follows an Endocytic Pathway*—*S. pyogenes* triggers an endocytic pathway that efficiently delivers invasive M3 streptococci into lysosomes (13) of endothelial cells. Thus, to identify the route of internalization and destina-

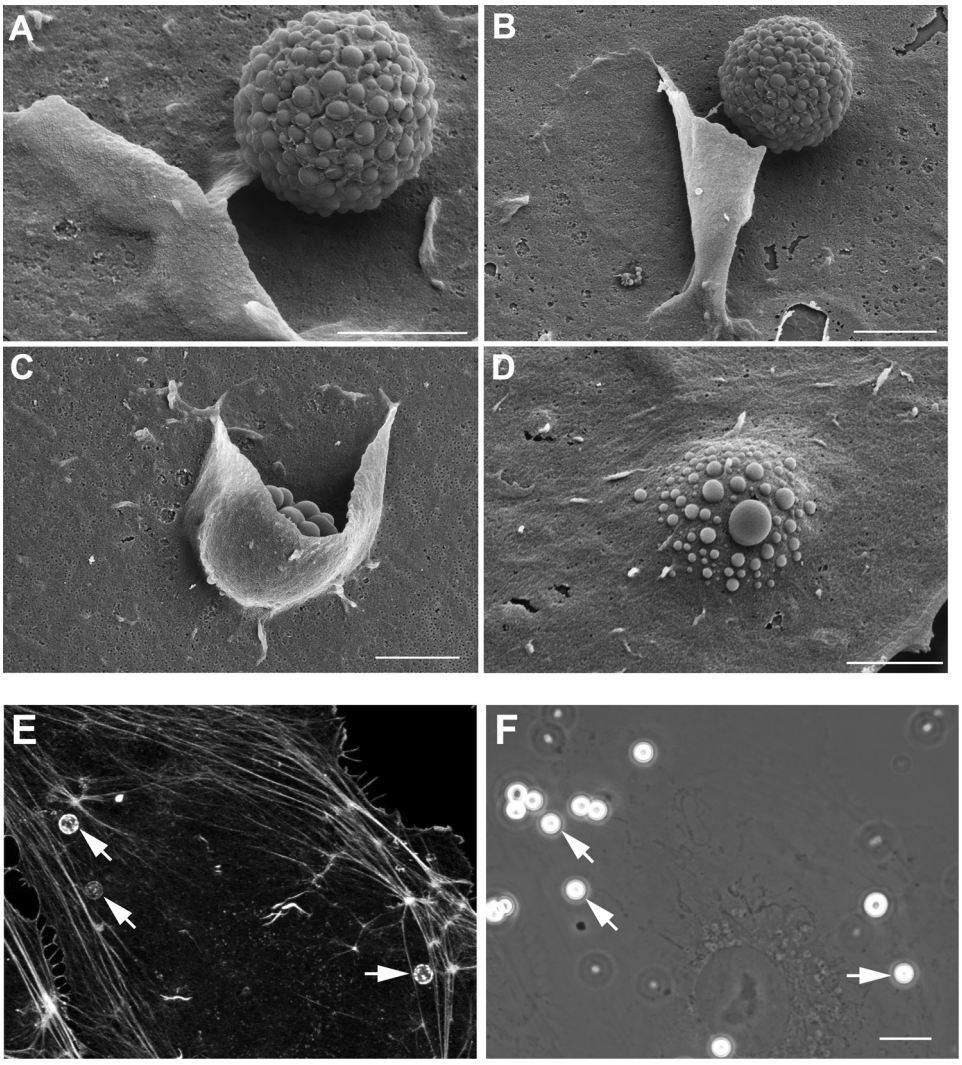


FIGURE 4. **SpyCep induces cytoskeletal rearrangements during uptake.** *A–D*, scanning electron microscopic images of SpyCep-coated beads being internalized into HUVEC. Extracellular beads are taken up by a zipper-like mechanism characterized by the formation of membrane protrusions. *Bars* represent 2 $\mu$m. *E* and *F*, confocal maximum intensity projection of SpyCep-coated beads that show accumulation of F-actin arrows, (*E*) and the corresponding phase contrast image (*F*). *Bar* represents 10 $\mu$m.

tion of SpyCep-mediated uptake, we tested whether SpyCep-coated beads also follow the classical endocytic pathway. Immunostainings of beads and the early endosomal marker EEA1 and the late endosomal/lysosomal marker protein Lamp-1 were conducted at early (60 min) and later stages (120 min) of co-incubation. Immunofluorescence microscopic analysis revealed the presence of internalized SpyCep beads in an EEA1-positive compartment at early time points (Fig. 5*A*, *arrow*). After 120 min of incubation, the majority of beads were found to be localized in a Lamp-1-positive compartment (Fig. 5*B*). Because the 3-$\mu$m bead size itself may influence the sorting direction of the beads, SpyCep was coupled to 15-nm gold particles, revealing a pseudo-soluble fraction of SpyCep. This pseudo-soluble form of the protein allowed us to visualize uptake and trafficking of SpyCep in HUVEC. As for the SpyCep beads, SpyCep-gold particles were efficiently taken up into HUVEC and delivered to lysosomes (Fig. 5, *C–E*). Within lysosomes, gold particles no longer reacted with the anti-SpyCep antibody, revealing the loss of antigenicity or dissociation of SpyCep within lysosomes. This indicates that SpyCep mediates its uptake and subsequent trafficking via the classical endocytic pathway with lysosomal destination.

*SpyCep Does Not Act as Invasin on the Bacterial Surface*—To address the question whether SpyCep may act as an invasin on the streptococcal surface, we constructed a SpyCep hyperexpressing *S. agalactiae* strain by transforming it with the previously described plasmid pCepA (5). Flow cytometry analysis was conducted to quantify the amount of surface located SpyCep on the constructed strain, as well as on the GBS control strain. As shown in supplemental Fig. S1, SpyCep-expressing *S. agalactiae* (GBS-SpyCep) showed a 50-fold stronger fluorescent signal as compared with the M3 *S. pyogenes* strain A475 and a more than 100-fold increase in fluorescence as compared with the GBS control strain (GBSpDCerm). This result demonstrates that the GBS-SpyCep construct is a hyperexpressing strain with an even higher content of surface-associated SpyCep than the M3 *S. pyogenes* strain. However, in contrast to the M3 *S. pyogenes* strain, GBS-SpyCep showed no invasion activity on HUVEC (data not shown). Moreover, analysis of the invasion potential of the SpyCep knock-out A475 *S. pyogenes* strain revealed an equal uptake rate as compared with the A475 wild-type strain (data not shown). Thus, it may be concluded that SpyCep does not act as an invasin on the streptococcal surface.

*A Blocking Antibody for SpyCep-mediated Internalization*—Purified anti-rSpyCep IgG or non-immune rabbit IgG was added to rSpyCep-coated beads prior to co-incubation with HUVEC. Only SpyCep-specific antibodies significantly blocked internalization of beads into HUVEC, but not the control rabbit IgG antibodies (Fig. 6). When anti-SpyCep antibodies were tested for their ability to interfere with the IL-8-degrading activity of SpyCep, the antibodies had no effect (data not shown), further strengthening the concept that cellular interaction and IL-8 degradation are two distinct functions displayed by this important virulence factor of *S. pyogenes*.

## DISCUSSION

*S. pyogenes* is a strict human pathogen in which a variety of multifunctional virulence factors have evolved. For example, C5a peptidase, structurally related to SpyCep, is a multifunc-

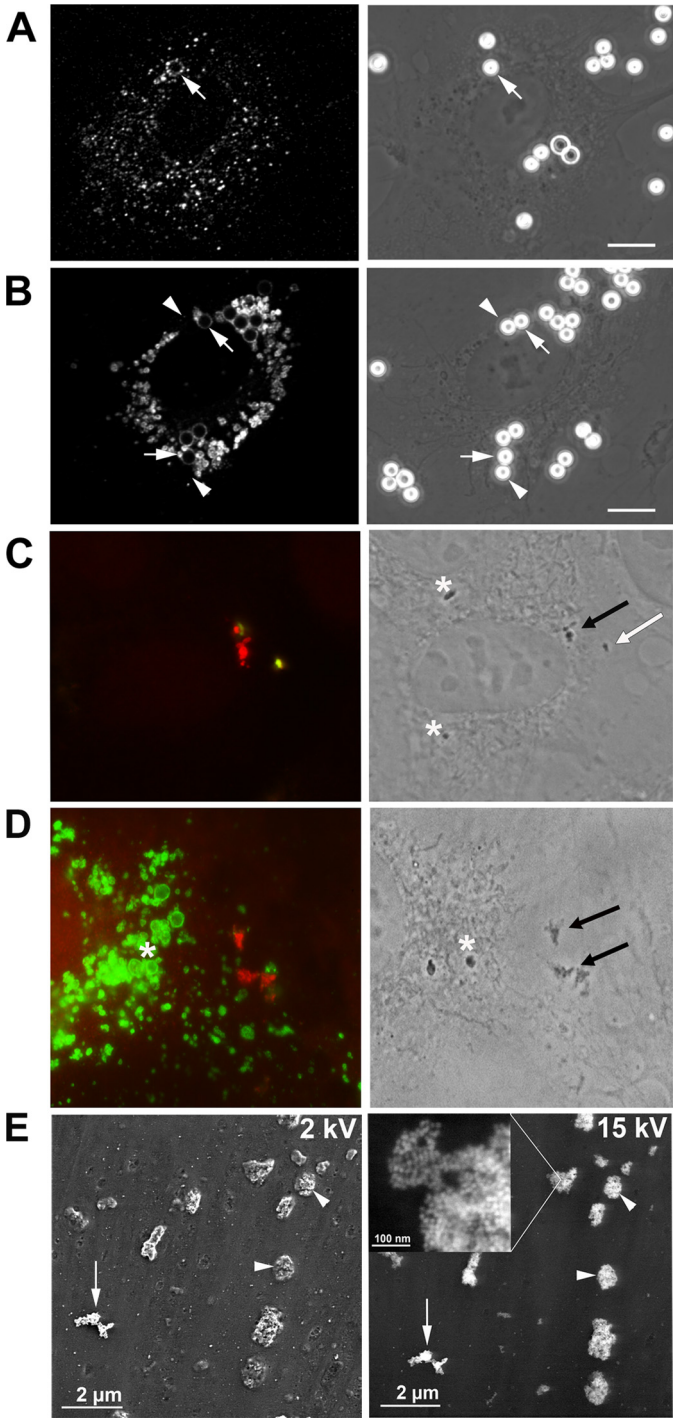


FIGURE 5. **SpyCep mediates uptake via the classical endocytic pathway.** *A*, accumulation of EEA1 in the vicinity of rSpyCep-coated internalized latex beads (*arrow*). *B*, internalized beads are delivered to Lamp-1-positive compartments. *Arrows* exemplify Lamp-1 accumulation around beads, whereas *arrowheads* point to beads within non-maturated phagosomal compartments. Single confocal sections are shown. *Bars* represent 10 μm. *C*, internalization of pseudo-soluble SpyCep-gold into HUVEC (extracellular SpyCep-gold is *green*, and intracellular SpyCep-gold is *red*). The *right panel* shows phase contrast image (*white arrow* shows extracellular gold particle, and *black arrow* shows intracellular gold; reactivity with the anti-SpyCep antibody). *D*, Lamp-1 stain of SpyCep-gold particles in HUVEC (*black arrows* show internalized SpyCep-gold particles, and *asterisks* indicate gold particles within lysosomes that lost anti-SpyCep reactivity. *E*, scanning EM of SpyCep gold particles internalized by HUVEC. At low voltage (2 kV, *left panel*), extracellular gold particles appear brighter (*white arrow*) than intracellular gold particles (*arrowheads*). At higher voltage (15 kV, *right panel*), the *inset* shows single internalized gold particles at higher resolution. *Bars* represent 5 μm.

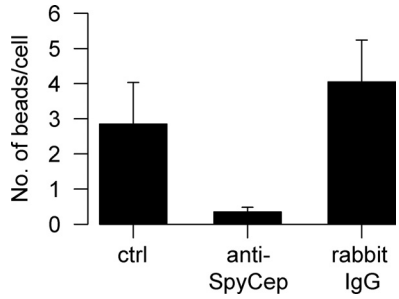


FIGURE 6. **Inhibition of invasion of rSpyCep-coated latex beads into HUVEC by anti-SpyCep antibodies.** SpyCep beads were first preincubated with rabbit polyclonal anti-SpyCep antibodies for 1 h and then co-incubated with HUVEC for 2 h. Preincubation of SpyCep-coated beads with anti-SpyCep IgG completely abolished the adherence to and invasion of SpyCep-coated beads into HUVEC. Non-immune rabbit IgG served as control (*ctrl*). Graph represents mean ± S.D.

tional *S. pyogenes* surface protease, shown to possess C5a-degrading activity but also adhesive functions, independent from the enzymatic activity (14). In the present case of SpyCep, only one biochemical function had been previously recognized: the ability to specifically bind and cleave C*X*C chemokines, one of which is IL-8. In published animal studies, a clear consequence of SpyCep expression has been improved survival and greater tissue spreading of the bacteria during the course of necrotizing soft tissue infection (3–5). We here demonstrate cloning, expression, and purification of full-length mature SpyCep in its enzymatically active form. This polypeptide served as a starting molecule for designing further C- and N-terminal truncations that allowed defining the minimal domain required for IL-8 degradation. A recent study also attempted to express active recombinant SpyCep (15); however, recombinant enzymatic activity was only obtained by combining two recombinant subfragments of SpyCep. This is in contrast to our findings, as confirmed both by quantitative IL-8 degradation assay and by Western blot analysis, that full-length mature SpyCep (excluding the predicted pre-pro-domain) was enzymatically active and was being expressed as one polypeptide (Fig. 1). Furthermore, the C-terminally truncated subfragment (PR+A, lacking 521 amino acid residues of the C terminus as well as the pre-pro-domain) was sufficient to cleave IL-8 (Figs. 2 and 7). These data further characterize the chemokine-degrading function of SpyCep.

The human endothelium is an important cellular barrier through which IL-8 is transported and on which it becomes exposed through binding to glucosaminoglycans to function in leukocyte recruitment (16–18). Here we analyzed the invasion activity of SpyCep using a latex bead-based internalization assay, which previously led to the discovery of many potent bacterial invasins 19–22), as well as pseudo-soluble SpyCep coupled to 15-nm gold particles. The results demonstrate that SpyCep specifically mediates its own uptake into endothelial cells via an endosomal pathway and that the PR domain is required but also sufficient to mediate cell entry (Figs. 5 and 7). The question arises whether SpyCep is an invasin. Our results indicate that SpyCep, expressed on the surface of GBS, does not mediate streptococcal invasion. Moreover, inactivation of the SpyCep-encoding gene in M3 *S. pyogenes* had no effect on the invasion potential. To fulfill the function of an invasin, SpyCep

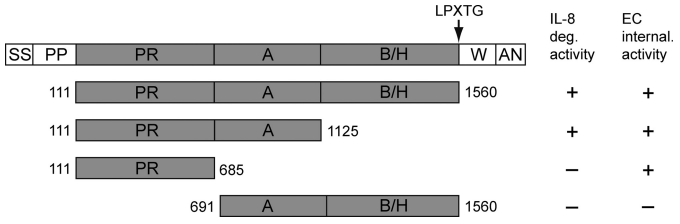


FIGURE 7. **Schematic overview of the domain structure of SpyCep.** The recombinant SpyCep fusion peptides generated in this work and their IL-8-degrading activity (*IL-8 deg. activity*) and endothelial cell invasion activity (*EC internal. activity*) are displayed. Amino acid residue positions are given for each fragment (according to accession number ABA33824.1).

has to be surface-exposed and covalently linked to the streptococcal cell. However, secreted derivatives of SpyCep lack the C-terminal part of the protein (3), indicating post-translational processing events that may be responsible for the loss of the N-terminal invasion-mediating PR domain in its surface-anchored form. Moreover, a very recent publication demonstrated that SpyCep is autocatalytically processing its N terminus, leading to the generation of an N-terminal cleavage product that non-covalently assembles to the C-terminal part and assembles to an active protease (23). Interestingly, the cleavage side resides within the PR domain between residues 244 and 245, demonstrating that the N-terminal part of the PR domain is no longer covalently linked to the peptidoglycan. These findings may thus explain why SpyCep does not act as an invasin, even if it is hyperexpressed in the GBS system. Our interpretation is that SpyCep is potent in mediating its own internalization into HUVEC but may not be considered as an invasin of *S. pyogenes*.

One key observation was that SpyCep impairs neutrophil recruitment from bloodstream to the tissue site of infection by inactivating IL-8 (3–5, 24). IL-8 produced by extravascular cells (macrophages, fibroblasts) must traverse the EC barrier from tissue site of infection to the luminal side of the endothelium to exert its promigratory effect on neutrophils (16). SpyCep produced at the tissue site may efficiently degrade IL-8 locally and thus prevent EC transcytosis and luminal presentation. However, EC are also able to produce and secrete endogenous IL-8. This EC IL-8 will not be exposed to the tissue site but will be directly transported to and presented at the luminal side of the EC barrier. Thus, the ability of SpyCep to promote its specific uptake into EC may represent a key event for interaction of SpyCep with EC-derived IL-8 or the endothelial barrier itself.

*Acknowledgment—We thank N. Janze for excellent technical assistance.*

## REFERENCES

1. Sumby, P., Whitney, A. R., Graviss, E. A., DeLeo, F. R., and Musser, J. M. (2006) *PloS. Pathog.* **2,** e5
2. Siezen, R. J. (1999) *Antonie Van Leeuwenhoek* **76,** 139–155
3. Edwards, R. J., Taylor, G. W., Ferguson, M., Murray, S., Rendell, N., Wrigley, A., Bai, Z., Boyle, J., Finney, S. J., Jones, A., Russell, H. H., Turner, C., Cohen, J., Faulkner, L., and Sriskandan, S. (2005) *J. Infect. Dis.* **192,** 783–790
4. Hidalgo-Grass, C., Mishalian, I., Dan-Goor, M., Belotserkovsky, I., Eran, Y., Nizet, V., Peled, A., and Hanski, E. (2006) *EMBO J.* **25,** 4628–4637
5. Zinkernagel, A. S., Timmer, A. M., Pence, M. A., Locke, J. B., Buchanan, J. T., Turner, C. E., Mishalian, I., Sriskandan, S., Hanski, E., and Nizet, V. (2008) *Cell Host Microbe* **4,** 170–178
6. Hidalgo-Grass, C., Dan-Goor, M., Maly, A., Eran, Y., Kwinn, L. A., Nizet, V., Ravins, M., Jaffe, J., Peyser, A., Moses, A. E., and Hanski, E. (2004) *Lancet* **363,** 696–703
7. Sumby, P., Zhang, S., Whitney, A. R., Falugi, F., Grandi, G., Graviss, E. A., Deleo, F. R., and Musser, J. M. (2008) *Infect. Immun.* **76,** 978–985
8. Eran, Y., Getter, Y., Baruch, M., Belotserkovsky, I., Padalon, G., Mishalian, I., Podbielski, A., Kreikemeyer, B., and Hanski, E. (2007) *Mol. Microbiol.* **63,** 1209–1222
9. Perez-Casal, J., Price, J. A., Maguin, E., and Scott, J. R. (1993) *Mol. Microbiol.* **8,** 809–819
10. Talay, S. R., Zock, A., Rohde, M., Molinari, G., Oggioni, M., Pozzi, G., Guzman, C. A., and Chhatwal, G. S. (2000) *Cell. Microbiol.* **2,** 521–535
11. Rohde, M., Müller, E., Chhatwal, G. S., and Talay, S. R. (2003) *Cell. Microbiol.* **5,** 323–342
12. von Köckritz-Blickwede, M., Goldmann, O., Thulin, P., Heinemann, K., Norrby-Teglund, A., Rohde, M., and Medina, E. (2008) *Blood* **111,** 3070–3080
13. Nerlich, A., Rohde, M., Talay, S. R., Genth, H., Just, I., and Chhatwal, G. S. (2009) *J. Biol. Chem.* **284,** 20319–20328
14. Cheng, Q., Stafslien, D., Purushothaman, S. S., and Cleary, P. (2002) *Infect. Immun.* **70,** 2408–2413
15. Fritzer, A., Noiges, B., Schweiger, D., Rek, A., Kungl, A. J., von Gabain, A., Nagy, E., and Meinke, A. L. (2009) *Biochem. J.* **422,** 533–542
16. Middleton, J., Neil, S., Wintle, J., Clark-Lewis, I., Moore, H., Lam, C., Auer, M., Hub, E., and Rot, A. (1997) *Cell* **91,** 385–395
17. Webb, L. M., Ehrengruber, M. U., Clark-Lewis, I., Baggiolini, M., and Rot, A. (1993) *Proc. Natl. Acad. Sci. U.S.A.* **90,** 7158–7162
18. Witt, D. P., and Lander, A. D. (1994) *Curr. Biol.* **4,** 394–400
19. Martinez, J. J., Mulvey, M. A., Schilling, J. D., Pinkner, J. S., and Hultgren, S. J. (2000) *EMBO J.* **19,** 2803–2812
20. Dersch, P., and Isberg, R. R. (1999) *EMBO J.* **18,** 1199–1213
21. Braun, L., Ohayon, H., and Cossart, P. (1998) *Mol. Microbiol.* **27,** 1077–1087
22. Molinari, G., Talay, S. R., Valentin-Weigand, P., Rohde, M., and Chhatwal, G. S. (1997) *Infect. Immun.* **65,** 1357–1363
23. Zingaretti, C., Falugi, F., Nardi-Dei, V., Pietrocola, G., Mariani, M., Liberatori, S., Gallotta, M., Tontini, M., Tani, C., Speziale, P., Grandi, G., and Margarit, I. (2010) *FASEB J.*, in press
24. Kurupati, P., Turner, C. E., Tziona, I., Lawrenson, R. A., Alam, F. M., Nohadani, M., Stamp, G. W., Zinkernagel, A. S., Nizet, V., Edwards, R. J., and Sriskandan, S. (2010) *Mol. Microbiol.* **76,** 1387–1397